

Article

Diel and seasonal patterns in water quality continuously monitored at a fixed site on the tidal freshwater Potomac River

R. Christian Jones* and Alexander P. Graziano

Potomac Environmental Research and Education Center, George Mason University, 4400 University Dr, MSN 5F2, Fairfax, VA 22030 USA

*Corresponding author email: rcjones@gmu.edu

Received 20 February 2013; accepted 4 August 2013; published 26 September 2013

Abstract

Recent advances in water quality monitoring have facilitated the acquisition of temporally rich datasets that allow comprehensive analysis of patterns and underlying processes and drivers at multiple scales. We analyzed data from a continuous water quality monitor on the tidal Occoquan River, a tributary of the tidal Potomac River and Chesapeake Bay. Temperature, conductivity, dissolved oxygen (DO), and pH were collected at 15 minute intervals from April through early November of 2010. Results of time series analysis indicate that, on a short-term basis, conductivity manifested an underlying semidiel pattern, presumably driven by tidal excursion. In comparison, DO, pH, and temperature exhibited a diel pattern correlated with the daily light and temperature cycle. Longer-term patterns were related to longer-term climatic factors such as a dry summer with low freshwater inputs, seasonal progressions of light and temperature, and a river discharge spike in early October. Examination of multiday patterns in DO and pH using 15 minute data during a climatically stable period illustrated both diel and semidiel patterns. Patterns in a period of strong hydrological forcing revealed a disruption of diel and semidiel patterns for several days with a general restoration of patterns thereafter. Both diel and seasonal data suggest that abundant submerged aquatic vegetation in the study area was the main primary producer component driving diel and seasonal DO and pH patterns.

Key words: continuous monitoring, dissolved oxygen, pH, specific conductance, submersed aquatic vegetation, temperature, temporal variation, tidal

Introduction

Recent advances in water quality monitoring have facilitated “continuous monitoring,” the acquisition of basic water quality variables at fixed locations at short intervals over extended periods. The datasets derived from these deployments can be used to enhance our understanding of the effect of driving variables like light, freshwater inflows, and temperature on water quality dynamics in tidal waters as well as the interplay among water quality parameters. Basic water quality parameters such as water temperature, specific conductance (or salinity), dissolved oxygen (DO), and pH can determine the suitability of inland and coastal habitats for aquatic life. Water quality standards exist for temperature, DO, and pH because these parameters can be affected by pollution and other

stressors. Some aquatic species important to ecosystem structure and function may exist at or near their temperature and DO tolerances (Moore and Jarvis 2008). Continuous monitoring can provide a more detailed and complete picture of the exposure of organisms to potentially stressful water quality conditions. In addition, detailed information on diel variations in water quality variables such as DO and pH can provide information on biological processes like photosynthesis and respiration.

The tidal Potomac River is part of the Chesapeake Bay tidal system, the largest estuary on the east coast of North America and one of the most productive coastal systems in the world. Historically, the system was characterized by lush beds of submersed aquatic vegetation (SAV) and numerous productive fisheries such as oysters, blue crabs, shad, and rockfish. These resources and their associated

supporting ecosystems have suffered large declines, with water quality degradation being a key stressor in this process (Breitburg et al. 1997, Orth et al. 2010). SAV virtually disappeared from the tidal freshwater Potomac River by the mid-20th century but has partially recovered in some areas to regain some of its status as an important ecosystem component (Carter and Rybicki 1986).

Diel variation in DO and pH has been assessed in the tidal freshwater Potomac in relation to phytoplankton blooms and SAV beds using lower intensity sampling regimes than those provided by continuous monitoring. Employing 90 minute interval data collected at shallow water sites, Carter et al. (1988, 1991) concluded that DO and pH fluctuations outside SAV beds were affected by both SAV and phytoplankton photosynthesis due to tidal water movement. Jones (1991) used 2 hour interval data to document very large diel swings in DO and pH attributable to blooms of the cyanobacterium *Microcystis aeruginosa* in open water areas of Gunston Cove, another embayment of the tidal freshwater Potomac River. Jones (1990) examined the response of temperature, DO, pH, and chlorophyll to tide stage and time of day at sites located inside and outside of SAV beds in the Dogue Creek embayment of the tidal freshwater Potomac. DO and pH fluctuations were large and attributable to both SAV and high densities of phytoplankton in the surrounding water, which was swept into the beds at high tide. Using dye and flow meter studies, Rybicki et al. (1997) demonstrated the substantial movement of water from SAV beds into the river channel area in the tidal freshwater Potomac. All of these studies were short term, and none addressed issues of seasonal variation and hydrological forcing. The longer sampling intervals also made it difficult to resolve differences between diel (solar cycle induced) and tidal influences.

The goals of this study were (1) to examine the patterns of water quality variability in this shallow water system at various scales ranging from subdiel through seasonal and (2) to relate patterns to climatic, hydrologic, and biologic drivers. At short time scales under stable weather conditions, we hypothesized that basic water quality variables such as temperature, specific conductance, DO, and pH would follow either diel or semidiel patterns (or both) based on responsiveness to semidiel tidal forcing and/or diel solar radiation forcing. Diel radiation forcing could be either direct for some variables such as temperature or indirect via photosynthesis for DO and pH. Under certain transient perturbations like freshwater inflow events, these short-term cyclical patterns may be temporarily dampened or may disappear completely for a time. At a longer time scale, we hypothesized that changes in water quality would be attributable to some combination of gradual seasonal changes in solar

radiation and gradual, or perhaps sudden, event-driven changes in freshwater inflow into the tidal system.

Study site

The Potomac River is one of the major subestuaries of the Chesapeake Bay system with a watershed area of 29,940 km² at the head of tide. Tidal influence on the Potomac River extends a distance of about 160 km from its confluence with the main bay at Point Lookout to Chain Bridge at the western boundary of Washington, DC. Due to substantial inflow of freshwater into the tidal Potomac, freshwater conditions (<0.5 ppt salinity) are generally maintained through Quantico, Virginia, about 50 km downstream of the head of tide, although in dry summers brackish conditions can extend slightly further upstream (Lippson et al. 1981). A significant volume of freshwater is diverted from the river for domestic use just above the head of tide, and a roughly corresponding large volume of treated sewage enters the tidal river, most of it just below Washington, DC. The freshwater tidal Potomac has had a history of substantial blooms of the cyanobacterium *Microcystis aeruginosa* (Jones 1991). Dramatic decreases in phosphorus loading due to sewage treatment plant upgrades have greatly decreased the frequency and severity of these blooms since 2000 (Jones 2008).

Data analyzed in this paper were from a continuous water quality monitor on the tidal Occoquan River at the Belmont Bay development in Woodbridge, Virginia, USA (38.6558°N, 77.2321°W). This monitor is part of the Potomac On-line Data System (PODS) deployed and maintained by the Potomac Environmental Research and Education Center of George Mason University (<http://perc.gmu.edu/pods.html>). With a watershed area of 1476 km² (<http://www.owml.vt.edu>), the tidal Occoquan River is a major tributary of the tidal Potomac River located about 40 km downstream from the head of tide. Fall line flow from the tidal Occoquan is controlled by a dam located just upstream from the head of tide, which creates the Occoquan Reservoir, a major drinking water supply for northern Virginia. Releases from the dam occur during wet periods, but substantial intervals of no discharge may occur. The tidal Occoquan is located in the lower portion of the tidal freshwater zone about 10 km upstream of the general boundary between tidal fresh and brackish waters in the tidal Potomac at Quantico, Virginia.

Methods

Temperature, conductivity, DO, and pH were collected at 15 minute intervals from April through mid-November of 2010 using YSI 6600 extended deployment sondes. The sondes were equipped with a copper-coated probe cover

and wiping brush parts, and individual probes were wrapped in copper-impregnated tape to minimize fouling. The sonde was moored in a perforated PVC stilling well attached to a floating dock at a constant depth of about 0.6 m immediately adjacent to the main channel of the tidal Occoquan. This channel is maintained for boat traffic to a depth of 3 m, but there was no dredging during the study period. A moderate amount of boat traffic was present on a daily basis, but tidal water movement was probably a greater factor in water mixing and turbulence. There is little or no depth stratification in this area, and tides are semidiurnal with amplitudes of about 0.6 m. During 2010, SAV developed in the extensive shallows both upstream and downstream of the monitor site (Fig. 1). Data were transmitted to a dedicated web site maintained by YSI and at weekly intervals were emailed to the investigators.

Two sondes were rotated at the deployment site at monthly intervals, at which time sondes were cross-checked for comparability. Due to the extended deployment, quality control and assurance procedures were important to ensure data comparability as sondes were rotated. Before deployment, sondes were calibrated in the lab against known standards as per manufacturer's guidance (YSI 2009); calibration of sondes was also checked upon return to the laboratory.

On site, before deployment, the to-be-installed sonde (outgoing sonde) was deployed adjacent to the current, soon-to-be removed sonde (incoming sonde), and a set of readings was made using the handheld readout and the outgoing sonde. Simultaneously, a water sample was taken for lab analysis. The incoming sonde was then retrieved, unhooked from the monitor, and the outgoing sonde was substituted. The incoming sonde was then deployed adjacent to the newly installed outgoing sonde, and a set of measurements was taken with the handheld readout and the incoming sonde. A second water sample was then collected for lab analysis. A light profile was collected by measuring photosynthetically active radiation (PAR) levels at 10 cm intervals in the top meter of the water column using an LI-COR LI-192 underwater sensor. A second PAR probe was used to track changes in ambient light during the underwater profiling. Secchi disk depth was determined.

Known volumes of the 2 water samples were filtered in duplicate through ashed and tared glass fiber filters (Whatman 984AH) for solids analysis. Total suspended solids (TSS) was determined by drying the filters at 75 °C overnight and reweighing. Volatile suspended solids (VSS) was subsequently determined by ashing the filters at 500 °C and reweighing. VSS was the difference between dry weight and ash weight. Chlorophyll *a* was determined by filtration through 0.45 µm membrane filters

followed by subsequent extraction in DMSO-acetone and fluorometry (Jones et al. 2008).

Sonde data were combined at the end of the year into one large file containing the water quality at 15 minute intervals for the entire study period. Data quality was insured by examining both the degree to which the

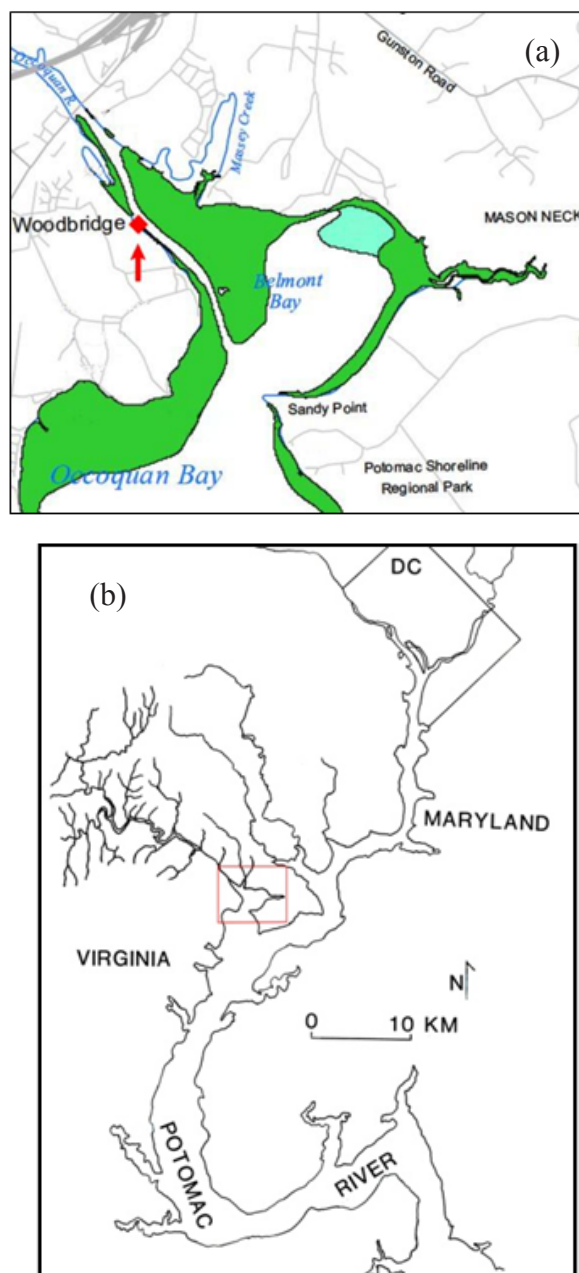


Fig. 1. Tidal Potomac River study site: (a) local area showing continuous monitor location (red square) and SAV coverage (heavy coverage: green, darker shading; moderate coverage: blue, lighter shading). From Orth et al. 2011; (b) vicinity map showing upper tidal Potomac River (local area map covers area of small red rectangle.).

incoming sonde had maintained its calibration and the comparability of data collected at the site before and after sonde change-out, as noted above. The following sonde change tolerances were met: temperature ± 0.2 °C; specific conductance ± 0.025 mS/cm; DO (% saturation) $\pm 3\%$; and pH ± 0.2 pH units. Data quality was also assessed by establishing acceptable data ranges for given parameters and censoring data outside these ranges; temperature could not be >35 °C, and specific conductance could not be >5 mS/cm. All specific conductance values >1 mS/cm were examined more closely to see if they were part of a longer pattern or a single- or short-term outlier. DO (% saturation) could not be $>200\%$, and DO (mg/L) could not be <2 mg/L; pH could not be >11 or <5 . Values were also checked to see if they doubled or halved between each 15 minute interval with the assumption that a doubling or halving was unrealistic and indicative of a sonde error. Few data abnormalities were observed using these criteria, and all were easily resolved. For every sonde change there was a 15 minute gap in the data, which was remedied by averaging the values from 15 minutes before and 15 minutes after.

Weather data (air temperature and PAR) were collected at 15 minute intervals at the deployment site using a Hobo weather station from Onset Computer. In addition to the original 15 minute temporal scale, data were compiled as daily averages. Occoquan River flow data were obtained from the web site of the Occoquan Watershed Monitoring Laboratory (<http://www.owml.vt.edu>). Daily means, ranges, medians, maxima, and minima were calculated for each day for all parameters (including discharge). SAV coverage for 2010 (Fig. 1) was obtained from the annual aerial survey report compiled by the Virginia Institute for Marine Science (Orth et al. 2011); graphing was done using SigmaPlot 11.2; statistical analyses were done with Systat 13; correlation analysis utilized the nonparametric Spearman coefficient; and time series analysis was conducted using Systat's Time Series Autocorrelation command. In this analysis, each value is correlated with succeeding values at each time step into the future. Correlation generally decreases as number of time steps increase, but if a variable has cyclical behavior, correlation will peak at a certain number of time steps into the future, allowing the periodicity of the cycling to be determined.

Results

Monthly grab sample data

Solids, chlorophyll *a*, and light transparency data were collected on a monthly basis when sondes were changed out (Table 1). Samples collected before and after

deployment were similar on each date, so only the average is shown. TSS was generally in the range of 4–8 mg L⁻¹, with higher values in spring ranging up to 17.3 mg L⁻¹. VSS was less variable with values from 1.8 to 3.8 mg L⁻¹. VSS constituted 19–48% of TSS with lower percentages in spring. Chlorophyll *a* ranged from 1.8 to 8.6 µg L⁻¹ and pheopigment from 3.7 to 6.6 µg L⁻¹; transparency was greatest in summer and least in spring; Secchi disk depth ranged from 0.84 m in April to 1.67 m in July; and light attenuation coefficient ranged from 1.16 m⁻¹ in June to 2.18 m⁻¹ in April. There was a negative correlation between Secchi disk depth and TSS ($r = -0.853$, $P < 0.01$), a somewhat lower and marginal correlation between Secchi disk depth and VSS ($r = -0.717$, $P < 0.05$), and a lack of correlation between Secchi disk depth and chlorophyll *a*, suggesting that nonalgal solids, particularly inorganic solids, controlled water transparency.

Seasonal patterns in climatic and hydrologic variables using daily averages

Seasonal patterns in climatic and hydrologic forcing variables (Fig. 2) were determined from daily mean values. Occoquan River inflow (Fig. 2a) was low or zero on most days, punctuated by short periods of higher inflow. Inflow to the tidal area was determined by releases from the Occoquan Reservoir immediately upstream from head of tide. Small runoff events in the watershed were offset by water withdrawals from the reservoir and did not result in appreciable releases; however, if input into the reservoir was great enough, water was released downstream into the tidal Occoquan River.

Two events of major freshwater inflow from the reservoir were observed during the study period. One was in late May with mean daily flows of 100 m³ s⁻¹ on 23 May, 120 m³ s⁻¹ on 24 May, and 36 m³ s⁻¹ on 25 May. Total inflow volume from these 3 dates was 22×10^6 m³. The second major inflow from the reservoir occurred at the beginning of October with mean daily flows of 36 m³ s⁻¹ on 30 September, 151 m³ s⁻¹ on 1 October, and 50 m³ s⁻¹ on 2 October, resulting in a total volume of 20×10^6 m³ from this 3 day event. For reference, the volume of the entire tidal Occoquan Bay/River complex including extensive areas downstream of the study site is 35×10^6 m³ (Lippson et al. 1981); thus, both of these events were capable of flushing most of the water from the tidal area around the monitoring site and replacing it with reservoir water.

While the Occoquan River inflow provides an appreciable part of the fresh water input to the tidal Occoquan in the area of the monitor, the fall line flow of

the mainstem of the Potomac River provides the bulk of the water that fills the upper tidal Potomac mainstem and blocks the movement of brackish water upriver. Interestingly, during 2010 the Potomac fall line flow pulses occurred at similar times as those in the Occoquan River (Fig. 2b). The late May Occoquan flow pulse was accompanied by a tripling of Potomac River fall line flow. The strong late September–early October Occoquan River flow event was matched with a major increase in flow at the Potomac fall line.

Average daily PAR values (Fig. 2c) demonstrated a maximum in late June around the time of summer solstice and then followed a general decline for the remainder of the year. Clear and partly cloudy days followed the upper, seasonally decreasing trajectory with mostly cloudy days dipping well below. An appreciable number of these cloudy days occurred in mid-August and late September–early October.

From an initial value of about 15 °C at the beginning of April, air temperature exhibited a general seasonal increase through the end of June, reaching a maximum of 25–30 °C in July (Fig. 2d). Average daily temperatures exhibited a gradual decline in August and then more strongly decreased through mid-November reaching about 10 °C. Individual daily means were often up to ± 5 °C from the fitted trend line and seemed to follow a multiday cycle.

Seasonal patterns in monitor data using daily averages

Daily mean water temperature followed seasonal trends similar to those for daily mean air temperature (Fig. 2e). The multiday cycle was also evident, but the amplitude of the cycle for water temperature was less, with values generally ≤ 3 °C from the trend line. Daily mean water temperature exceeded 30 °C on 22 days as opposed to 8 days for daily mean air temperature.

Specific conductance remained at low values (about 0.3 mS), well within the range for fresh water, from April through mid-July (Fig. 3a). The one slight increase in that period occurred in the immediate wake of the late May reservoir discharge event. A major surge in specific conductance representing incursion of brackish water from downriver in the tidal Potomac started in mid-July, continued through August, and then intensified through September, reaching a maximum of 1.46 mS on 28 September. A dramatic decline was observed in the following days, with values declining to 0.40 mS by 2 October as flow from the Occoquan pushed the brackish water back down river, aided by increased Potomac fall line flows.

Average daily DO measured in percent saturation was

relatively high (>100%) in early April, declining somewhat through April and May to values slightly below 100% (Fig. 3b). This was followed by an increase to values above 120% in late June and into early July. A second decline was noted through July and August to values consistently below 100%, which remained through most of the remainder of the study period. An exception was an obvious multiday surge in DO to well above the trend line in early October in the immediate aftermath of the second upstream flow event.

Trends in average daily pH were similar to those in DO, with lower values (<8.0) in the April through May period followed by a clear increase to higher values (>8.0) during June, which were maintained through July. A decline was observed in August reaching the lower values (<8.0) for the rest of the year. The same multiday increase seen in DO in early October in the wake of the second reservoir flow event was also noted for pH.

Correlation analysis of daily means

Correlation analysis of daily means was conducted to assess significant relationships among the variables. All correlations were based on 224 data pairs except those involving PAR, which were limited to 163 data pairs. As expected, water temperature and air temperature were highly correlated ($r = 0.903$, $P < 0.001$). Daily averages of pH ($r = 0.674$, $P < 0.001$) and PAR ($r = 0.633$, $P < 0.001$) were also highly correlated with those of air temperature. Owing to its sporadic nature, Occoquan River discharge was not strongly correlated with water quality variables on an ongoing daily basis. Both daily average pH and DO were strongly related to daily PAR ($r = 0.604$, $P < 0.001$ and $r = 0.526$, $P < 0.001$, respectively); however, the relationships with PAR became even stronger when they were related to daily range in pH and DO ($r = 0.646$, $P < 0.001$ and $r = 0.741$, $P < 0.001$, respectively). The relationship between pH and DO was also improved by correlating daily ranges ($r = 0.826$, $P < 0.001$) versus daily averages ($r = 0.571$, $P < 0.001$).

These results warrant the further examination of seasonal patterns in daily ranges of DO and pH because they may more accurately reflect daily photosynthesis than the average values of these parameters (Fig. 4). The daily range in both of these variables exhibited a clear seasonal pattern increasing from April through June and then slowly but consistently decreasing through the remainder of the study period. DO range varied from about 20% saturation in April and October to $\geq 60\%$ saturation in late June; pH ranges were typically about 0.5 units early and late in the year and >1.0 unit during late June and into July.

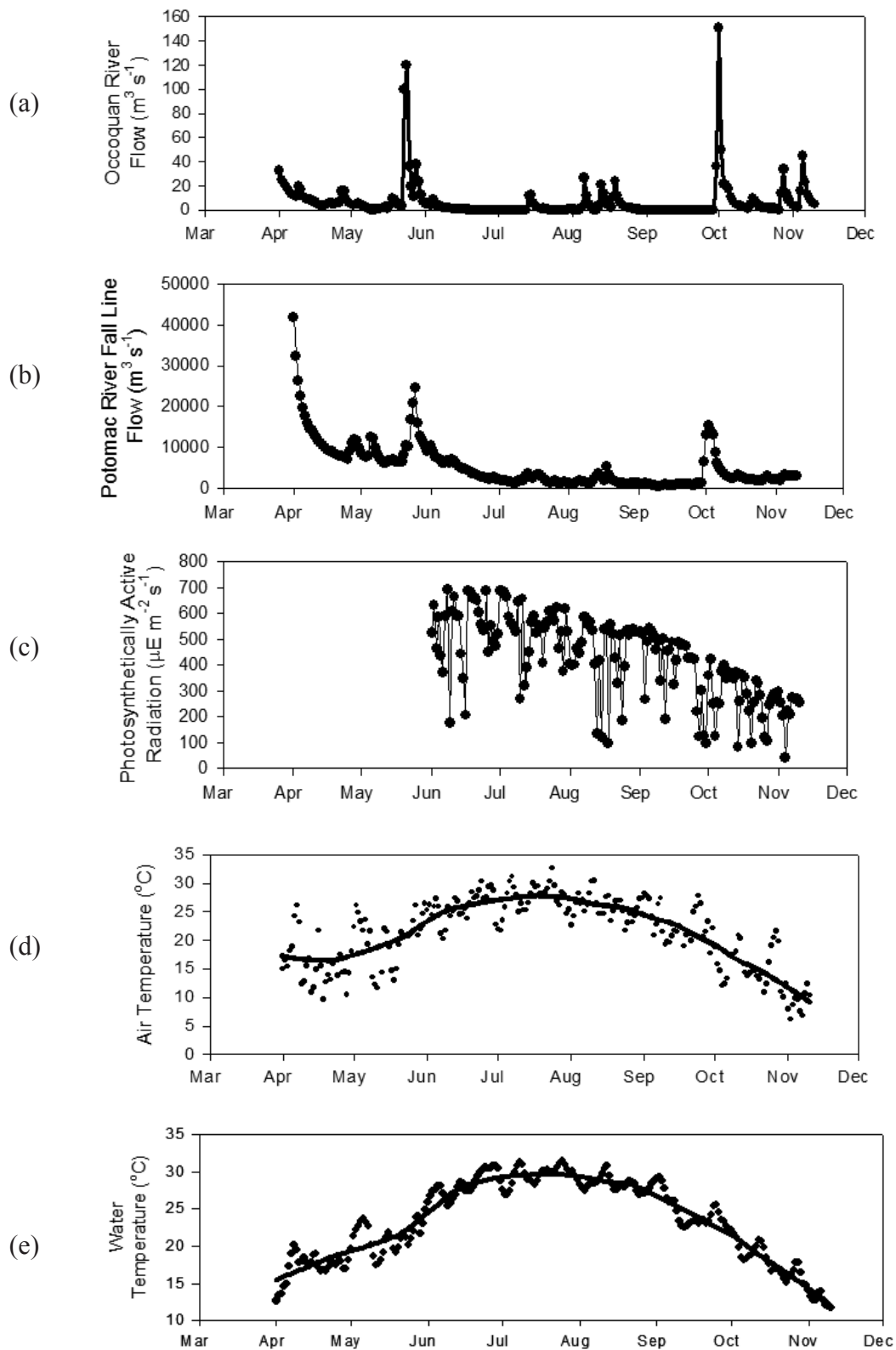


Fig. 2. Daily mean values for climatic and hydrologic forcing variables. Lines for temperature graphs were obtained by LOWESS with a tension (f) of 0.2. River flow lines and PAR line connect daily mean values. Month tick is first day of month.

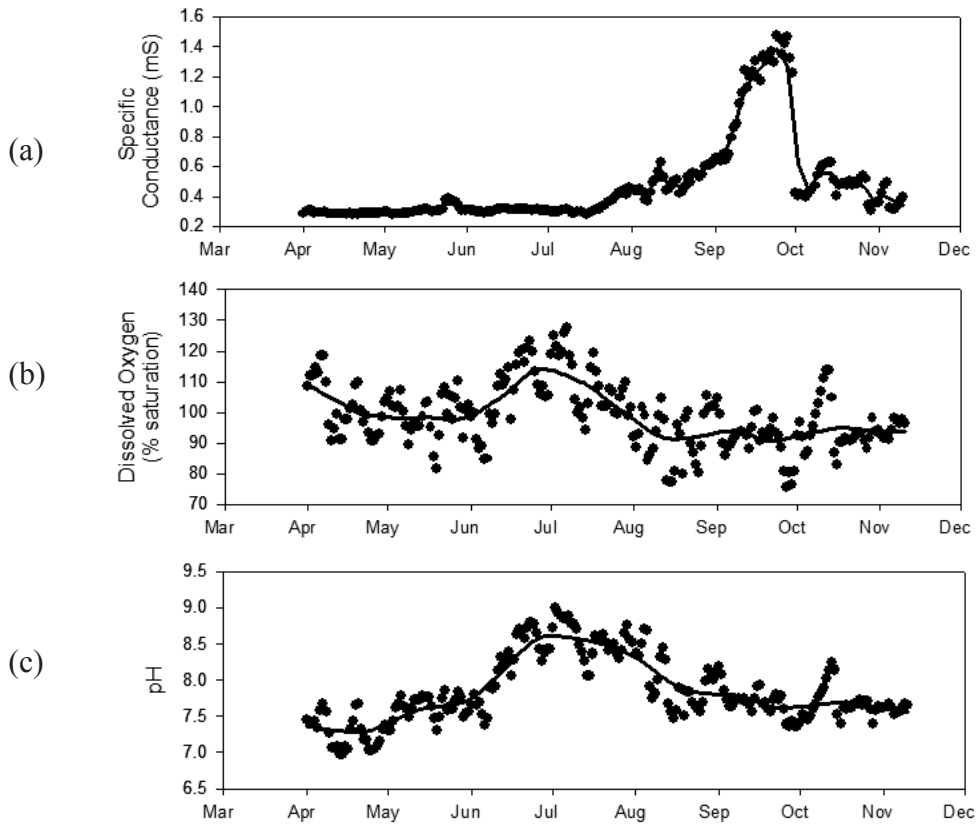


Fig. 3. Daily mean values for water quality parameters. Lines for all graphs were obtained by LOWESS. For LOWESS, tension (f) was 0.2 except for specific conductance, where f was 0.05. Month tick is first day of month.

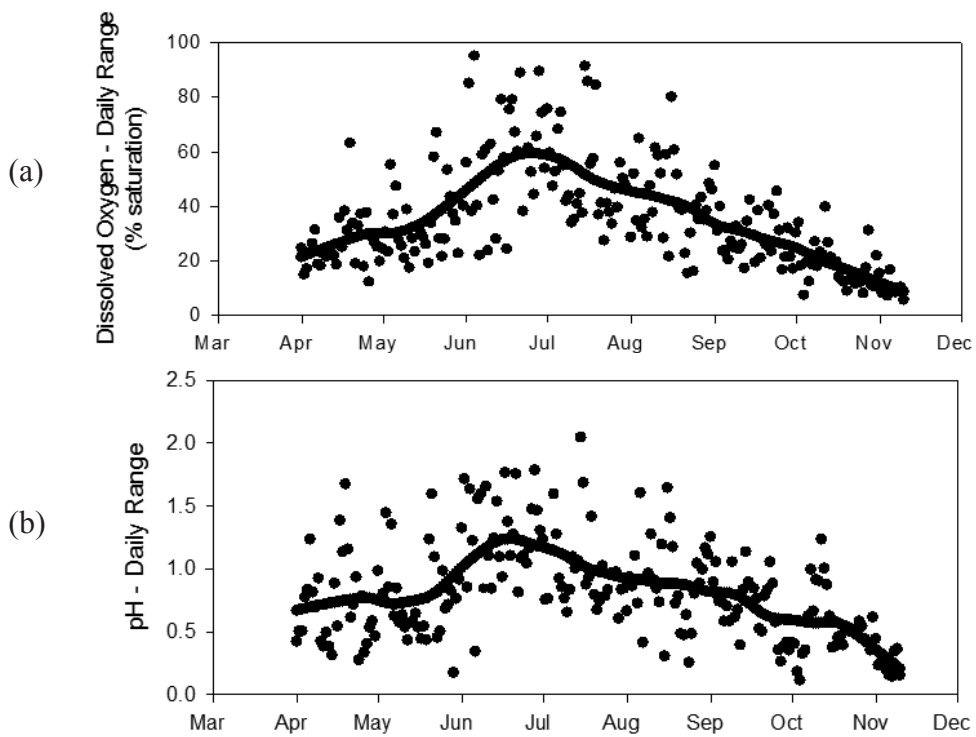


Fig. 4. Daily range for dissolved oxygen and pH. Trend line is LOWESS fit with tension (f) = 0.2. Month tick is first day of month.

Table 1. Monthly grab sample data collected while changing sondes.

Date	Secchi Depth (m)	TSS (mg L ⁻¹)	VSS (mg L ⁻¹)	Chl (ug L ⁻¹)	Pheo (ug L ⁻¹)	Light Attenuation Coefficient (m ⁻¹)
1Mar2010	----	17.3	3.3	2.44	3.66	—
1Apr2010	0.84	11.2	3.8	6.86	6.59	2.18
3May2010	0.98	9.1	2.4	5.67	4.87	1.48
4Jun2010	1.40	6.3	2.6	1.77	3.95	1.16
9Jul72010	1.67	5.2	2.0	7.37	5.02	1.21
11Aug2010	1.62	6.3	2.3	6.59	4.61	—
8Sep2010	1.58	5.7	2.7	7.33	5.16	—
5Oct2010	0.94	7.9	2.9	8.57	6.25	1.53
10Nov2010	1.60	4.9	2.2	—	—	—
3Dec2010	1.52	7.8	1.8	2.11	3.77	—

Table 2. Summary of Autocorrelation Analysis for 15 minute data.

Month	Short Term (<1 day) Autocorrelation Patterns				
	Water Temp	Specific Cond	pH	DO (% saturation)	DO (mg L ⁻¹)
April	D-MA	IRR	D-HA	D-HA	D-MA
May	D-MA	SD-LA	D-HA (SD-LA)	D-HA	D-HA
June	D-MA	SD-HA	D-HA (SD-LA)	D-HA	D-HA
July	D-MA	SD-MA	D-HA	D-HA	D-HA
August	D-MA	SD-HA	D-MA	D-HA	D-HA
September	D-LA	SD-MA	D-MA (SD-LA)	D-HA	D-HA (SD-LA)
October	D-LA	SD-MA	SD-MA	D-HA	D-MA

Symbols: D = diel pattern, SD = semidiel pattern, IRR = Irregular pattern, HA = high amplitude (autocorrelation varies by >0.4 per cycle), MA = medium amplitude (autocorrelation varies by 0.1–0.4 per cycle), LA = low amplitude (autocorrelation varies by <0.1 per cycle); patterns in parentheses are secondary in amplitude to main pattern.

Diel patterns from individual 15 minute readings: time series analysis

Diel patterns in water temperature, specific conductance, DO, and pH were probed using time series analysis of the 15 minute data. In this case the lag interval is 15 minutes so that a 24 hour diel period would consist of 96 lag units.

As expected, air temperature and PAR exhibited autocorrelation plots indicative of diel patterns (Fig. 5a and b). In both cases correlation coefficients declined to a minimum after 48 lag units (12 h) and increased to high values after 96 lag units (24 h), clearly indicating a cyclical pattern with a period of 24 hours. This pattern continued to repeat with only a small decay in correlation peaks. Water temperature followed a pattern of autocorrelation virtually identical to that of air temperature (Fig. 6a).

The autocorrelation of DO and pH also followed a diel pattern similar to that of temperature and PAR with a minimum at 12 hours and a maximum at 24 hours (Fig. 6c

and d). A different pattern was observed for specific conductance with the autocorrelation plot showing minima at 6 and 18 hours and maxima at 12 and 24 hours (Figure 6b). This pattern was characterized as semidiel, synchronized to the semidiel tidal regime in the study area. Interestingly, pH showed a slight secondary maximum at 6 and 18 hours, suggesting a possible secondary tidal effect.

To determine if the autocorrelation signals were consistent throughout the year, data were segmented by month, and autocorrelation of 15 minute data was repeated for each water quality parameter and month (Table 2). Water temperature and DO showed a consistent diel pattern in autocorrelation with high to moderate amplitude. Specific conductance exhibited the semidiel pattern in all months except April when an irregular pattern was observed. Highest amplitude of the pattern was found in June and August. When broken down by month, pH continued to demonstrate a strong diel pattern, but in some months (May, Jun, and Sep) a semidiel pattern was also evident at lower amplitude.

Diel patterns from individual 15 minute readings: 2 selected periods

To further examine the timing of diel and semidiel patterns in water quality relative to solar and tidal cycles, relevant parameters were plotted for 2 selected periods of 12–14 days each. We selected one period in June during relatively stable conditions and a second period from late September to early October in the wake of the large flow event discussed earlier.

The last 2 weeks in June were a period of relatively stable climatic conditions (Fig. 7). PAR was near optimal every day being near summer solstice and with no cloudy days. At the beginning of the period (17 Jun), maximum PAR (noon) coincided with high tide (Fig. 7a). By 24 June maximum PAR was at low tide, and by 30 June noon again coincided with high tide. Mean water temperature gradually increased during the period from about 27 °C on 17 June to nearly 31 °C by 23 June (Fig. 7b). It remained stable through 29 June and then declined on 30 June. The daily cycle was consistent during the period, with a range of about 1.5–2 °C, closely and consistently related to the diurnal solar cycle. Highest temperatures were reached in the late afternoon regardless of tide stage. In comparison, specific conductance was closely tied to the tidal cycle (Fig. 7c). Specific conductance was always highest just at the time of high tide and lowest near the low tide time. On a few dates (e.g., 27 and 29 Jun), there was a slight secondary peak around low tide. During this stable period, there was little trend in daily average specific conductance. The amplitude of daily variation was somewhat higher early in the period and declined slightly as the days went on.

DO and pH showed a clear relationship to the diurnal solar cycle, and little change in mean daily values was observed over this stable period (Fig. 7d and e). Maximum values of DO were generally observed in the late afternoon and minimum values around dawn. This pattern was distinct when late afternoon coincided with low tide (17 to 20 Jun); however, starting about 22 June, an increase in DO was observed earlier in the day coinciding with low tide, and this effect increased on 23 June to give a clear morning secondary peak. By 24 June, the morning (low tide) and afternoon peaks had merged giving a maximum around noon. As the tides continued to move later in the day, the DO peak migrated later in the day, but still remained in the afternoon when the solar radiation effect would be the greatest.

A similar pattern was seen for pH. Maximum pH values almost invariably occurred in late afternoon, and a secondary maximum related to low tide was also observed on 20 June and gradually increased. Again by 24 June the morning and afternoon peaks had merged; however, by 26 June the tide effect had produced a different outcome

suggested by, but not clearly evident in, the DO data: a midafternoon low tide pH peak and a second, post-midnight low tide pH peak with a late afternoon, early evening pH minimum. This pattern continued through 30 June, suggesting a source of high pH and DO water sweeps into the area at low tide.

Examination of short term water quality dynamics during the late September to early October flow event also yielded interesting results (Fig. 8). PAR levels showed more day to day variability than in June, with 3 distinctly cloudy days (29 and 30 Sep and 4 Oct) and some partly cloudy days (5 and 6 Oct) in addition to a number of sunny days (Fig. 8a). The flow event that swept through the area in early October brought some major changes in water temperature patterns (Fig. 8b). First, the mean water temperature decreased strongly from about 23 °C on 29 September to about 18 °C by 6 October. Cloudy weather damped diurnal temperature patterns on 29 and 30 September. By 1 October flushing of resident water by the flow spike occurred (as evidenced by the specific conductance drop, noted below), and in subsequent days little diurnal variation in temperature was observed even on days of high PAR. By 5 October a daily pattern was again detectable, but in the first few days seemed to be more related to tide than solar cycle; highest values were found at low tide with a clear minimum at high tide. In the latter days of this period, temperature began to increase slightly, but the tidal effect was still evident.

Specific conductance was highly coupled to tide time before the flow event (Fig. 8c; 29 to 30 Sep). As the flow surge reached the tidal Occoquan at the monitor site, specific conductance patterns were disrupted in 2 ways. First, there was a dramatic drop in specific conductance values from well above 1 mS to about 0.4 mS. This occurred within a few hours on the evening of 30 September and was a good marker for the arrival of the flow spike waters at the monitor. Subsequently, the semidiurnal pattern disappeared completely for several days from 1 October to 4 October. A slight diurnal pattern appeared on 5 October and built over the next 2 days, reaching about the same magnitude (0.2–0.3 mS daily variation) as before the flushing event by 7 October.

Other parameters were also affected by the flow event, such as pH, which seemed to be more closely related to diurnal light cycle (Fig. 8e). On each date the maximum pH occurred in the latter half of each day and showed a clear relationship to the amount of PAR received during that day. For example, 29 and 30 September and 4 October were cloudy days, and on those days the pH peak was markedly reduced. On days with high amounts of solar radiation, 2 and 5–11 October, pH showed a strong afternoon peak. Exceptions were 1 and 3 October when high light did not produce much of a pH response, possibly

due to direct effects of the flow surge, such as flushing of phytoplankton from the area around the monitor or increased turbidity inhibiting SAV photosynthesis.

Another interesting pattern in the pH data was the emergence of a secondary peak early in the day from 6 to 10 October. This peak could not be explained by the solar cycle but was related to the occurrence of a morning high tide, which apparently brought higher pH water from down river. As the high tide moved later in the day, this morning peak started to merge with the afternoon maximum so that

by 10 October it became the shoulder of the larger afternoon peak. DO showed a similar pattern (Fig. 8d). Oxygen values showed a clear afternoon peak, the magnitude of which was related to the amount of PAR received. This pattern was muted in the aftermath of the flow event, but it became re-established starting on 5 October. A morning, tide-related increase was suggested from 7 to 10 October but was much less obvious than with the pH data. Note that starting on 5 October, both pH and DO began a multiday upward trend, which would continue through 13 October.

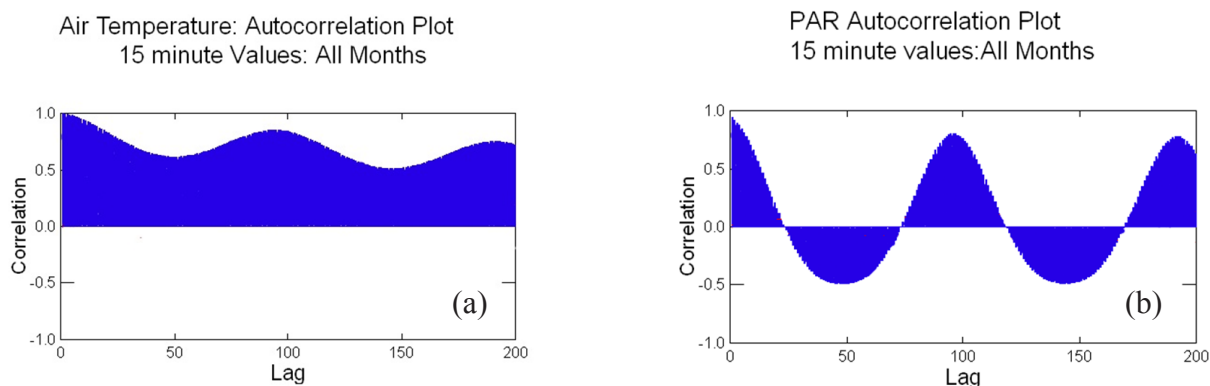


Fig. 5. Autocorrelation plots for forcing variables. Lag interval is 15 minutes. 96 lag units equal 24 hours.

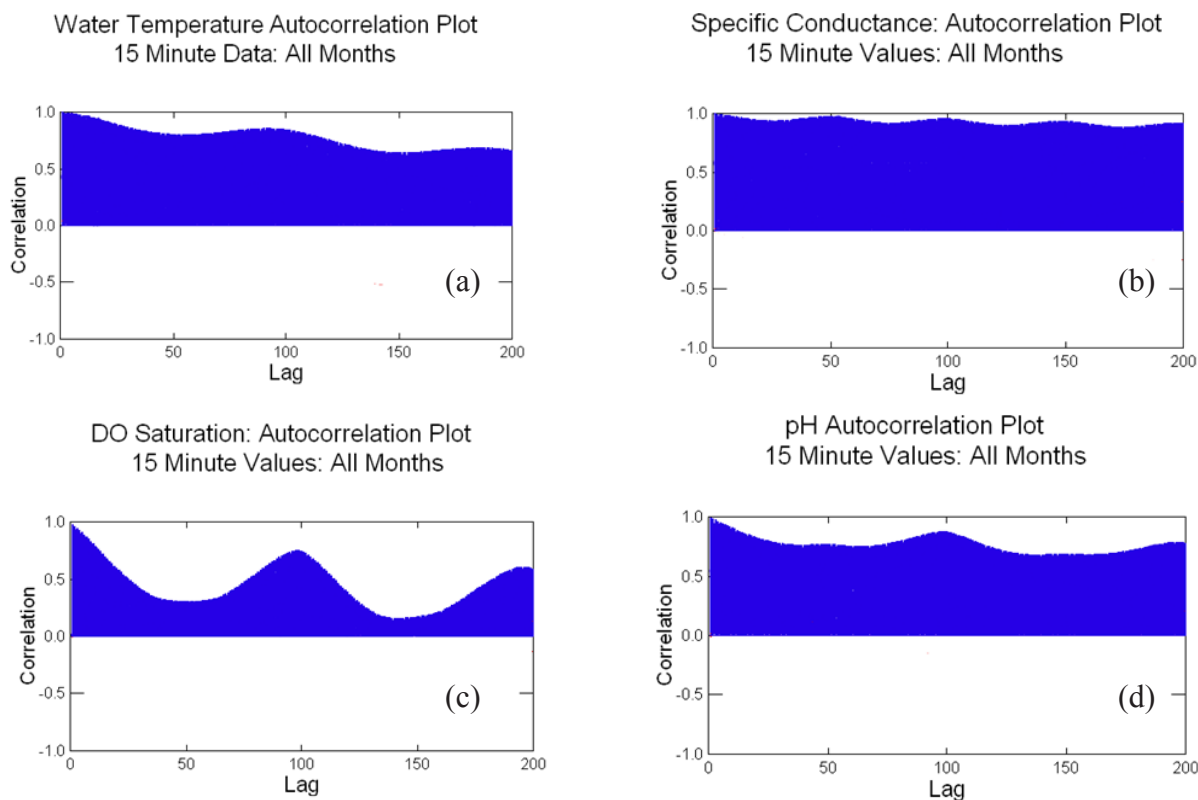


Fig. 6. Autocorrelation plots for water quality parameters. Lag interval is 15 minutes. 96 lag units equal 24 hours.

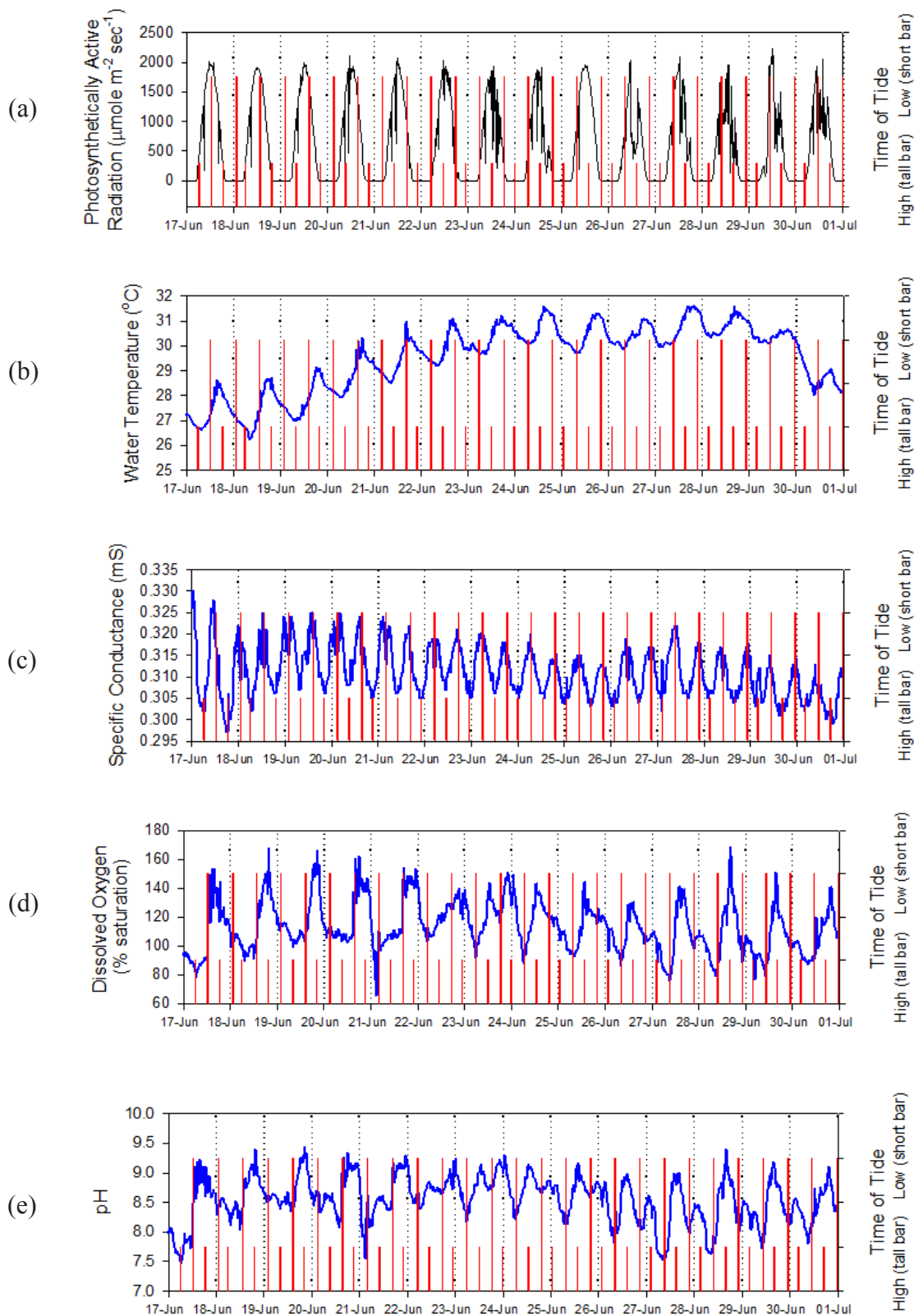


Fig. 7. Climatic and water quality variables in late June. Time of high and low tide indicated by tall and short bars, respectively. Vertical dotted lines are midnight beginning the day indicated below the tick: (a) photosynthetically active radiation ($\mu\text{mole m}^{-2} \text{s}^{-1}$); (b) water temperature ($^{\circ}\text{C}$); (c) specific conductance (mS); (d) dissolved oxygen (% saturation); (e) pH.

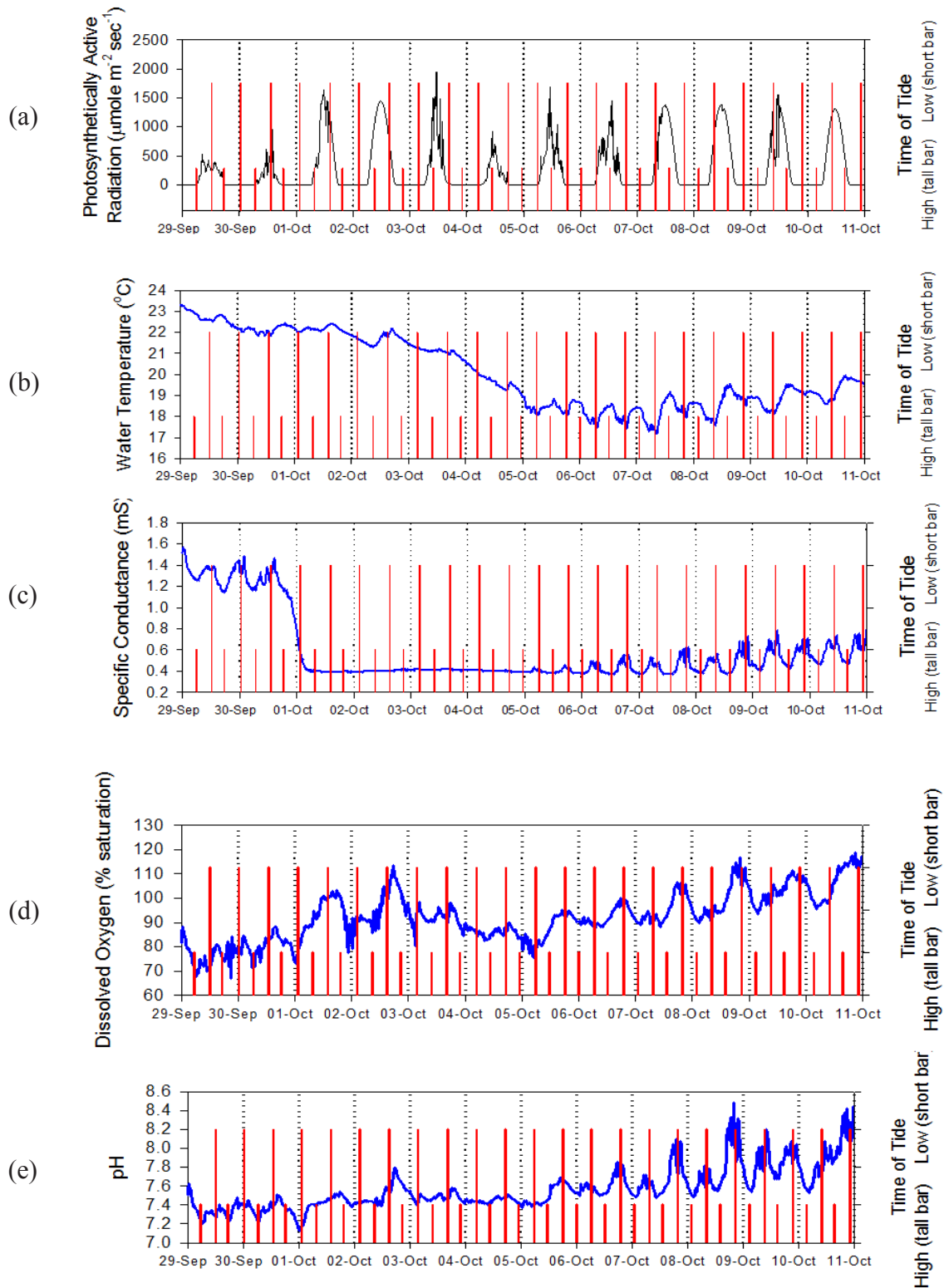


Fig. 8. Climatic and water quality variables in late September and early October. Time of high and low tide indicated by tall and short bars, respectively. Vertical dotted lines are midnight beginning the day indicated below the tick; (a) photosynthetically active radiation (PAR; $\mu\text{mole m}^{-2} \text{s}^{-1}$); (b) water temperature ($^{\circ}\text{C}$); (c) specific conductance (mS); (d) dissolved oxygen (% saturation); (e) pH.

Discussion

The first objective of this analysis was to determine patterns of water quality variability over a range of temporal scales. At short temporal scales under stable hydrologic and climatic conditions, the water quality variables examined exhibited clear and consistent diel or semidiel patterns related to solar and tidal cycles, respectively. This was shown by both autocorrelation analysis and close examination of a 14 day period of stable climatic and hydrologic conditions in late June. The relationship between the tidal cycle and the diurnal light cycle shifts daily with the tide times, advancing about 1 hour per day. Because there are 2 high tides and 2 low tides per day, over a period of about 6 days the time of maximum solar radiation (noon) will shift from low tide to high tide or visa versa. This potentially allows the disentanglement of tide effects from diurnal solar cycle driven effects, although other factors may intervene during this multiday shift.

Specific conductance was found to exhibit a clear semidiel pattern consistent with a tidal effect. This tidal effect on specific conductance was consistent with the findings from a range of National Estuarine Research Reserve System (NERRS) sites by Wenner and Geist (2001), who observed that salinity (as measured by specific conductance) exhibited a periodicity corresponding to tidal activity in all 9 estuarine sites studied ranging from Alabama to Virginia. Higher tides brought in water with slightly more ionic content and low tides restored lower ionic content water. Wilding et al. (2012), working at fixed sites in tidal freshwater systems in New Zealand, observed a more saline water mass at high tide. Other estuarine sites have also displayed a clear tide-related pattern to short-term variations in specific conductance (Edwards et al. 2004, Ward 2004, Necaie et al. 2005). Most, if not all, of these studies were conducted at sites that were more brackish, being at least oligohaline, while at the tidal Occoquan site values remained well within the freshwater range but continued to exhibit tide-related cycles in specific conductance.

Water temperature, DO, and pH all exhibited a strong diel pattern related to the solar cycle. Strong autocorrelations were found at lags of 24 and 48 hours for pH and DO. The strong diel DO signal observed here is consistent with the findings of Buzzelli et al. (2007) for a creek that had robust phytoplankton and a large marsh upstream. Given the tidal range of about 0.6 m in the tidal Occoquan, the dominance of the diel signal for DO is consistent with the findings of Wenner and Geist (2001) who found that diel periodicities were dominant for DO at a range of NERRS sites with lower tidal amplitudes.

The close relationship between PAR and both DO and

pH in the diel time series analysis and in the 15 minute data depicted for the periods in June and September–October strongly suggest a linkage mediated by photosynthesis of SAV, phytoplankton, or both. The monitor site is located in proximity to SAV beds both upstream and downstream on both sides of the river (Fig. 1). At its location on the edge of the river channel, the monitor is positioned to receive water from SAV beds during the frequent tidal water movements. SAV photosynthesis in the area would give a general diel pattern in DO and pH with highest values in late afternoon at the monitor. Further, under certain conditions this water movement would result in a semidiel signal if a concentrated mass of water from a nearby SAV bed moved through the monitor area. For example, water from a large SAV bed and tidal marsh just upstream on the same side of the river would be expected to spill out into the channel and flow past the monitor site as the tide goes out. This mechanism could easily explain the secondary semidiel signal in DO and pH as a result of elevated values of these variables at low tide, which was observed during the June stable period.

In addition to work cited earlier for the tidal Potomac, studies in a variety of waterbodies have found that SAV beds are capable of producing strong diel cycles in DO and pH levels. Caraco and Cole (2002), working in the tidal Hudson River, used continuous monitoring in macrophyte beds to document both diel variations in DO attributable to photosynthesis and respiration, but also semidiel effects related to tidal movements. Wilding et al. (2012) found that while diel forcing of DO related to SAV was dominant in tidal freshwater streams, semidiel tide-related effects were also important. Gruber et al. (2011) found strong enrichment in DO, pH, and temperature in Chesapeake Bay SAV beds during the day relative to nearby open water areas. Studies in inland freshwater systems have also demonstrated strong diel patterns in DO and pH in SAV beds. Frodge et al. (1990) found a strong diel signal in both pH and DO in submersed plant beds in Washington State, USA, lakes, which was most intense in midsummer. Continuous recording of DO in 2 Swiss streams demonstrated a strong diel oxygen pattern related to the presence of SAV (Kaenel et al. 2000).

Studies conducted in the tidal freshwater Potomac (e.g., Jones 1991) found that phytoplankton could be responsible for large diurnal swings in DO and pH under bloom conditions with chlorophyll levels near or above 100 $\mu\text{g L}^{-1}$. Given the rather modest chlorophyll levels observed in this study, however, phytoplankton were probably not a major factor in the observed diel patterns in DO and pH. Thus, several lines of evidence point to the abundant SAV in the area around the monitor as the major drivers of the observed seasonal and diel patterns in DO

and pH observed in this study and a source of DO, which is exported to surrounding open water areas.

At a longer seasonal temporal scale, clear and consistent patterns were observed in air temperature and PAR, generally reflected in gradual and somewhat predictable patterns in water quality variables. Due to the close occurrence of maximum PAR (late June) and maximum temperature (mid July) in 2010, it was difficult to clearly separate their effects; however, seasonal patterns in both DO and pH (daily mean and daily range) were more closely correlated with PAR levels, suggesting that PAR was more important in driving seasonal patterns. In other years such as 2009, the time separation of maximum PAR and maximum temperature was greater because the highest temperature was observed in mid-August (Jones and Buchanan 2009). This would allow for better discrimination of PAR and temperature effects at a seasonal scale.

While the seasonal patterns in DO and pH track seasonal changes in PAR in general, their decline during July and August is weaker than expected if only PAR was driving these variables. For example, a regression of DO against PAR for June showed a highly significant positive slope, whereas a similar analysis for July data was not significant. Clearly, the biomass and productivity of primary producers is also an important factor in the magnitude of daily DO and pH ranges. In the tidal Potomac, SAV continues to grow robustly and would be expected to continue to elevate DO and pH above saturation for the entire summer (Carter et al. 1988, 1991, Jones 1990). Kelly et al. (1983) observed similar seasonal shifts in the relationship between PAR and DO range in an SAV-dominated river. Thus, the seasonal patterns observed in DO and pH are consistent with SAV having a dominant role in the dynamics observed here.

During 2010, freshwater inflow at the Occoquan fall line was at or near zero for most days between early June and the end of September. This allowed brackish water to gradually mix with the ambient freshwater during this period. Specific conductance remained near 0.3 mS for the period from April through mid-July. Values increased steadily from mid-July through August and then rose sharply during September. This pattern was directly related to the timing of hydrological inputs. The extended dry period of summer 2010 allowed brackish water to slowly infiltrate the area at first and then come in more strongly as the drought continued into September. This incursion of brackish water was quickly expelled by the early October flow event. A somewhat different pattern was observed at this site in 2009 (Jones and Buchanan 2009). Specific conductance was only about 0.18 mS in early June of 2009. It increased steadily but slowly and reached only 0.35 by mid-September when data collection ended. The 2 years had different overall hydrology; 2010 was a dry year

with precipitation below normal from March through June whereas in 2009 precipitation was above normal for the same period and about 50% greater than in 2010. This resulted in lower spring specific conductance in 2009, and the higher salinity brackish water was never able to penetrate. In 2010 the low spring flows meant that the brackish water was not displaced as far downstream in the Potomac mainstem and was able to penetrate the study area during the prolonged summer drought.

An important objective of the study was to determine the role of transient perturbations such as major pulses of freshwater into the tidal area from adjacent watersheds. Freshwater inflow was relatively robust during the period of January to March of 2010, averaging about $50 \text{ m}^3 \text{ s}^{-1}$ with peaks as high as $280 \text{ m}^3 \text{ s}^{-1}$. During April and into May the Occoquan inflow decreased to low levels. During the long period between May and October, Occoquan and Potomac freshwater input was much reduced except for the 2 major inflow events in late May and late September–early October. As described earlier, both of these events were capable of flushing the Occoquan Bay area. The relative effect of the mainstem Potomac River fall line inflows on water quality at the fixed monitor was difficult to gauge in 2010 because they coincided closely with the local Occoquan inflows, but the local inputs were probably more important due their direct injection into the study area.

The late September–early October flow pulse had major consequences for water quality at the monitor. No flow had been released from the Occoquan dam during early and mid-September. As noted previously, discharge from the reservoir increased dramatically on 30 September, peaked on 1 October, and continued for several more days (Fig. 3a). PAR and air temperature both dropped during this period; however, within a few days of this water surge, PAR recovered to some extent and DO and pH began a steady increase, indicating that photosynthetic production was increasing. Diel variability in temperature, DO, and pH was disrupted for several days, and the semidiel pattern in specific conductance was eradicated for nearly 1 week. Specific conductance, which had increased strongly as brackish water penetrated before the flow event, was quickly reset to lower values. Water temperature began a steady decline of several days due principally to a decline in air temperature in the aftermath of the storm front. Given the large volume of tributary inflow from this event, the major changes were predictable; however, within 1 week after the flushing event, prestorm diel and semidiel patterns were clearly reemerging. DO and pH saw increased amplitude of diel patterns for about 1 week after reestablishment of these patterns.

The time for recovery of diel and semidiel patterns in water quality observed in the aftermath of the late September–early October flow event here was about 6–7

days; recovery in the May flow event was 3–4 days. Hubertz and Cahoon (1999) found recovery periods from 2 days to more than 1 week, depending on the size and timing of the runoff event. Ward (2004) examined the effect of one tropical storm and one hurricane and found that 1–2 weeks were necessary for recovery of semidiel salinity patterns from these large events.

In summary we found that diel cycles were dominant in temperature, DO, and pH variation at short time scales, while semidiel cycles attributable to tides were dominant for specific conductance at a fixed site in the tidal freshwater Potomac River. Tidally induced variation was also found in DO and pH on some occasions. At seasonal time scales, PAR was the dominant driver for DO and pH, whereas the seasonal pattern in water temperature was related to air temperature. At both short-term and seasonal time scales, patterns in DO and pH seemed to be driven by abundant SAV near the sample site. Seasonal patterns in specific conductance were related to the occurrence of freshwater flows into the study area. Following a several month period of essentially no freshwater input, brackish water gradually moved up into the area in late summer before being flushed out by a large flow event in late September. This flow event also profoundly, but temporarily, disrupted the diel and semidiel patterns in all parameters. These results inform our basic understanding of the degree and sources of variability of basic water quality parameters at a range of time scales.

Acknowledgements

We thank the Occoquan Watershed Monitoring Laboratory for providing data on Occoquan River discharge and water quality data from the Occoquan Reservoir. The Belmont Marina monitor is part of the Potomac Online Data System (PODS). PODS has been supported in part by grants from the Virginia Environmental Endowment, Chesapeake Bay Restoration Fund, the National Oceanic and Atmospheric Administration's B-WET Program, and George Mason University's College of Science. We thank Ken Moore at the Virginia Institute for Marine Science for sharing his QA/QC procedures for continuous monitoring. Publication of this article was funded in part by the George Mason University Libraries Open Access Publishing Fund.

References

- Breitburg DL, Loher T, Pacey CA, Gerstein A. 1997. Varying effects of low dissolved oxygen on trophic interactions in an estuarine food web. *Ecol Monogr*. 67:489–507.
- Buzzelli C, Holland A, Sanger D, Conrads P. 2007. Hydrographic characterization of two tidal creeks with implications for watershed land use, flushing times, and benthic production. *Estuar Coasts*. 30:321–330.
- Carico NF, Cole JJ. 2002. Contrasting impacts of a native and alien macrophyte on dissolved oxygen in a large river. *Ecol Appl*. 12:1496–1509.
- Carter V, Barko JW, Godshalk GL, Rybicki NB. 1988. Effects of submersed macrophytes on water quality in the tidal Potomac River, Maryland. *J Freshw Ecol*. 4:493–501.
- Carter V, Rybicki N. 1986. Resurgence of submersed aquatic macrophytes in the tidal Potomac River, Maryland, Virginia, and the District of Columbia. *Estuaries*. 9:368–375.
- Carter V, Rybicki NB, Hammerschlag R. 1991. Effects of submersed macrophytes on dissolved oxygen, pH, and temperature under different conditions of wind, tide, and bed structure. *J Freshw Ecol*. 6:121–133.
- Edwards D, Hurley D, Wenner E. 2004. Nonparametric harmonic analysis of estuarine water-quality data: a National Estuarine Research Reserve case study. *J Coastal Res*. 20:75–92.
- Frodge JD, Thomas GL, Pauley GB. 1990. Effects of canopy formation by floating and submergent aquatic macrophytes on the water quality of two shallow Pacific Northwest lakes. *Aquat Bot*. 38:231–248.
- Gruber RK, Hinkle DC, Kemp WM. 2011. Spatial patterns in water quality associated with submersed plant beds. *Estuar Coasts*. 34:961–972.
- Hubertz ED, Cahoon LB. 1999. Short-term variability of water quality parameters in two shallow estuaries of North Carolina. *Estuaries*. 22:814–823.
- Jones RC. 1990. The effect of submersed aquatic vegetation on phytoplankton and water quality in the tidal freshwater Potomac River. *J Freshw Ecol*. 5:279–288.
- Jones RC. 1991. Spatial and temporal patterns in a cyanobacterial phytoplankton bloom in the tidal freshwater Potomac River, USA. *Verh Internat Verein Limnol*. 24:1698–1702.
- Jones RC. 2008. Long term response of water quality to changes in nutrient loading at a mainstem site in the tidal freshwater Potomac River. *Verh Internat Verein Limnol*. 30:633–637.
- Jones RC, Buchanan C. 2009. Analysis of continuous water quality monitoring data from the tidal freshwater Potomac River. In: Fay P, editor. *Proceedings of 2009 Virginia Water Research Conference*. Blacksburg (VA): Virginia Water Resources Research Center; [cited 1 Oct 2011]. Available from: www.vwrrc.vt.edu/pdfs/proceedings/2009WaterResearchSymposium_proceedings_web.pdf
- Jones RC, Kelso DP, Schaeffer E. 2008. Spatial and seasonal patterns in water quality in an embayment-mainstem reach of the tidal freshwater Potomac River, USA: a multiyear study. *Environ Monit Assess*. 147:351–375.
- Kaenel BR, Buehrer H, Uehlinger U. 2000. Effects of aquatic plant management on stream metabolism and oxygen balance in streams. *Freshwater Biol*. 45:85–95.
- Kelley MG, Thyssen N, Moeslund B. 1983. Light and the annual variation of oxygen- and carbon-based measurements of productivity in a macrophyte-dominated river. *Limnol Oceanog*. 28:503–515.
- Lippson AJ, Haire MS, Holland AF, Jacobs F, Jensen J, Moran-Jonson

- RL, Polgar TT, Richkus WA. 1981. Environmental atlas of the Potomac estuary. Baltimore (MD): Johns Hopkins University Press.
- Moore KA, Jarvis JC. 2008. Environmental factors affecting recent summertime eelgrass diebacks in the Lower Chesapeake Bay: Implications for long-term persistence. *J Coastal Res (Special Issue)*. 55:135–147.
- Necaise A, Ross S, Miller J. 2005. Estuarine habitat evaluation measured by growth of juvenile summer flounder *Paralichthys dentatus* in a North Carolina estuary. *Mar Ecol-Prog Ser*. 285:157–168.
- Orth RJ, Williams MR, Marion SR, Wilcox DJ, Carruthers TJB, Moore KA, Kemp WM, Dennison WC, Rybicki N, Bergstrom P, Batiuk RA. 2010. Long-term trends in submersed aquatic vegetation (SAV) in Chesapeake Bay, USA related to water quality. *Estuar Coasts*. 33:1144–1163.
- Orth RJ, Wilcox DJ, Whiting JR, Nagey L, Owens AL, Kenne AK. 2011. 2010 distribution of submersed aquatic vegetation in Chesapeake Bay and coastal bays; [cited 1 Sep 2010]. Available from: http://web.vims.edu/bio/sav/sav10/index_draft.html
- Rybicki NB, Jenter HL, Carter V, Baltzer RA, Turtora M. 1997. Observations of tidal flux between a submersed aquatic plant stand and the adjacent channel in the Potomac River near Washington, DC. *Limnol Oceanog*. 42:307–317.
- Ward LG. 2004. Variations in physical properties and water quality in the Webhannet River Estuary (Wells National Estuarine Research Reserve, Maine). *J Coastal Res*. 45:39–58.
- Wenner EL, Geist M, 2001. The National Estuarine Research Reserves program to monitor and preserve estuarine waters. *Coast Manage*. 29:1–17.
- Wilding TK, Brown E, Collier KJ. 2012. Identifying dissolved oxygen variability and stress in tidal freshwater streams of northern New Zealand. *Environ Monit Assess*. 184:6045–6060.
- YSI, 2009. 6-Series Multiparameter Water Quality Sondes. User Manual. Revision E.